

DESIGN AND CHARACTERISTICS OF THE n_TOF EXPERIMENT AT CERN

D. Cano-Ott

On behalf of the n_TOF collaboration

CIEMAT

Avda Complutense 22, Madrid Zip: 28040, Spain

Abstract

The n_TOF is a 180 m long neutron time-of-flight facility being built at CERN [1]. The aim of the experiment is to measure with high accuracy neutron-induced reaction cross-sections in nuclei relevant to ADS and Transmutation, as well as to Astrophysics. The neutrons are produced by spallation in a massive lead target using the 20 GeV/c CERN-PS proton beam. It is foreseen that its operation will start by fall 2000. An overview of the design of installation will be reported, putting special emphasis on those aspects particular to the n_TOF: the excellent energy resolution and the high-energy spectrum of the neutrons.

Most of the samples relevant to ADS and transmutation are radioactive and available only in reduced amounts of high purity. This introduces some constraints to the beam optics that have to be considered. It will be shown how the design of the neutron beam line has been adapted to the sample dimensions, in order to preserve the features of the installation and at the same time allow clean experiments.

Another challenge in the n_TOF design is coming from its geometry. The beam line is located inside a closed tunnel, which has certainly a great impact in the reduction of the background. This becomes of particular importance in the attenuation of high-energy neutrons (up to several GeV), since they can traverse through large amounts of materials producing many secondary particles. It will be illustrated how the design of the collimation system and shielding elements along the beam line guarantees acceptable neutron and gamma backgrounds at the measuring station, providing in this way a clean environment for the detectors.

1. Introduction

Among the large number of topics relevant to the design of the n_TOF facility at CERN, a question of primary importance from the experimental point of view is the determination and definition of the characteristics of the installation. The time-of-flight (TOF) measurements require a geometrically well-defined neutron beam at the sample position and the absence of backgrounds. Moreover, the neutron beam has to be adapted to the size of the samples, which is limited by the available amounts of high purity materials, by the target construction procedure and also by their intrinsic radioactivity (in case of unstable isotopes). The neutron beam has to be compatible with the requirements coming from the various proposed experimental techniques. The experimental programme of the n_TOF project covers a wide range of measurements summarised as follows:

- (n,γ) cross-section measurements with C_6D_6 detectors (in a first phase) and with a total absorption 4π calorimeter (in the second phase).
- (n,f) cross-section measurements with **P**arallel **P**late **A**valanche **C**hambers (PPAC).
- (n,xn) cross-section measurements with Ge or Si detectors.

Even though many sources of background can be highly suppressed through the time-of-flight tagging, those background events having a time correlation similar to the neutrons may not be rejected and may severely distort the measurements. Such background sources can be classified in two categories: i) neutron reactions at the sample without the proper time-energy relation and ii) signals in the detectors (produced by photons, neutron recoils or other particles) not originating from the reaction under study. In the first case, the background can be highly reduced by designing the optical and shielding elements (beam tube, collimators and walls) of the neutron beam line. The second background species are also reduced in this way, but in addition the number of secondary reactions (of neutrons and charged particles) has to be minimised also at the experimental area and its vicinity. The n_TOF collaboration has dedicated a big effort to the studies needed for the definition of the neutron beam design. Such studies covered a large spectrum of issues that can be summarised as follows:

- Study of the neutronic properties of the spallation target. In particular, production rates, the energy, the time, the spatial and the angular distribution of the neutrons.
- Study and design of the beam optics, i.e. beam tube and collimators.
- Design of the necessary shielding elements, which guarantee clean experimental conditions.

It should be emphasised that all these investigations were made under the scope of providing optimal conditions to the measurements, according to the following directives:

- The neutron beam size should have a radius as small as 2 cm, given the availability of the samples, its intrinsic radioactivity, the overall detection efficiencies and the experimental requirements arising from the capture (both the C_6D_6 detectors and the 4π calorimeter), the fission and the (n, xn) measurements. However, further developments are considered in order to adapt the beam characteristics to particular measurements by studying and designing variable size collimators.
- Design the corresponding beam optics (beam tube and collimators) such as to achieve neutron and gamma backgrounds by order of magnitudes lower than the beam flux.
- Define the shielding elements such, as to improve the background attenuation and respect at the same time the conditions imposed by the CERN safety rules, which impose the accessibility and emergency escape paths of the installation.

The realisation of the present design implied complex and time consuming Monte Carlo simulations, in order to achieve quantitative solutions. Several codes based on different models and evaluated cross-section libraries, were used for this purpose (FLUKA [2], MCNPX [3], GEANT3 [4], GEANT4 [5] CAMOT [6] and EAMC [7]) and the results have been cross-checked among them, in order to asses their reliability. In this sense, our studies represent on themselves a benchmark between the most advanced codes available in neutron physics today.

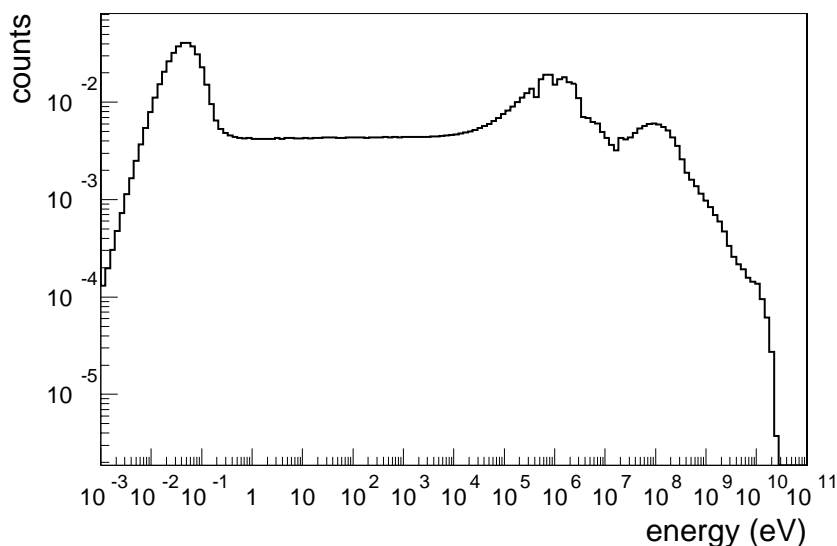
2. The spallation source

A detailed description of the properties of the lead spallation target can be found in [8]. This section is devoted only to those characteristics of the target that have an impact to the definition of the neutron beam. The study of the CERN neutron source had, among others, two major goals:

- To evaluate the most relevant properties of the spallation source, such as the flux and its spectral function.
- To parameterise these properties in order to implement them in time efficient, but realistic, Monte Carlo simulations, necessary for most of the studies.

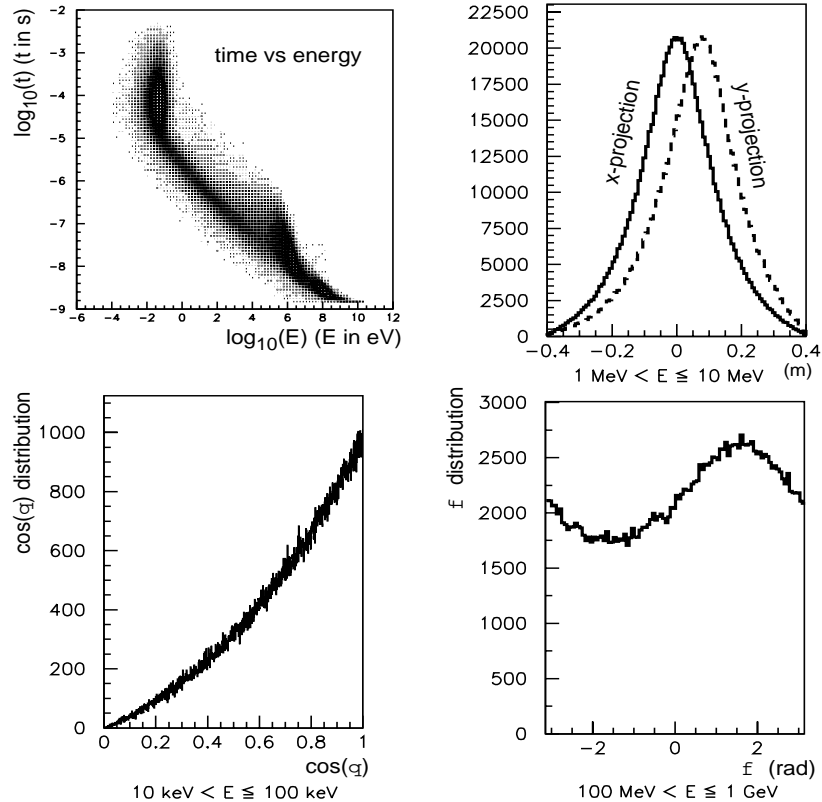
The neutron energies at the n_TOF extend closely up to 20 GeV due to the 20 GeV/c momentum of the PS proton beam. A FLUKA Monte Carlo simulated energy spectrum of the neutrons at the exit of the water moderator of the spallation target, is shown in Figure 1. The 38% of the neutrons emerge with energies below 0.3 eV. The range from 0.3 eV to 20 keV accounts for 23% of all neutrons and evidences almost exact isolethargic behaviour, as a consequence of the moderation in the water. However, a significant fraction 32% of the neutrons have energies between 20 keV and 20 MeV, and a further 7% extends above 20 MeV. Such a hard component, the signature of the spallation reactions, differentiates substantially the neutron energy distribution at the CERN facility from those of alternative neutron production mechanisms used in other neutron TOF facilities.

Figure 1. Energy distribution (normalised to area unity) of the neutrons at the exit of the Pb target after the water moderator



The simulation of the spallation process is excessively time-consuming for high-energy protons. An event generator appears to be necessary in order to perform effectively all calculations [9]. For this purpose, the interactions of the 20 GeV/c protons with the Pb spallation target ($80 \times 80 \times 40$ cm 3) were simulated by means of FLUKA [2] and EAMC [7]. A very detailed geometry of the target, the surrounding water moderator, the mechanical parts and the shielding was included. The position, energy, time and the direction cosines of the particles emanating entering into the TOF tube were recorded on a data summary tape (DST). We report here on the results obtained for the neutrons, but details about other emerging particles can be found in [8]. By taking the TOF tube as the z axis in a co-ordinate system, the proton beam lies in the y/z plane and enters into the target at $x = y = 0$ cm and $z = -40$ cm, forming an angle of $\theta = 10^\circ$ with respect to the z-axis. Such an incident angle balances the intensity losses in the neutron beam and its contamination due to high-energy charged particles, γ -rays and others. However, it introduces an asymmetry in the spatial distribution of the neutron source along the y-axis. The analysis of the DST provided the one-dimensional probability distributions of the neutron x- and y-positions, $p(x)$ and $p(y)$, the angular distributions of their momenta, $p(\theta)$ and $p(\phi)$, the time, $p(t)$, and the energy, $p(E)$, distributions. It was found that all single-variable distributions were strongly correlated with the neutron energy, and thus, its parameterisation was made as a function of the energy. Some illustrative examples can be found in Figure 2. In the upper left corner, the energy-time relation can be observed. Such relation is the working principle of the TOF measurements, since it links the time of flight with the initial neutron energy.

**Figure 2. Upper left: Time-energy relation of the spallation neutrons.
Upper right: x and y projections of the spatial distribution of neutrons
with energies between 1 MeV and 10 MeV. Lower left: $\cos(\theta)$ distribution for
neutron energies between 10 keV and 100 keV. Lower right: ϕ distribution for
neutron energies between 100 MeV and 1 GeV.**



In the upper right corner of Figure 2, the x and y spatial distributions for neutron energies between 1 MeV and 10 MeV are shown. Both distributions are clearly not uniform and present pronounced peaks with similar r.m.s. values. It can also be observed that the centroid of the y-distribution is displaced towards positive values, while the x-distribution remains centred in $x = 0$. The displacement varies with the neutron energy ranging from 4.1 cm, for energies below 1 eV, to 6.6 cm, for energies between 10 MeV and 100 MeV, and 9.8 cm for energies above 1 GeV. The r.m.s of both distributions presents also energy dependence. For neutron energies below 1 eV, a broad distribution is obtained with a r.m.s of 15.9 cm. The width reduces to 12.9 cm for energies between 1 MeV and 10 MeV and gets its smallest value of 5 cm for energies above 1 GeV.

In the lower left corner, the $\cos(\theta)$ distribution for energies between 10 keV and 100 keV is shown. It can be observed that the distribution is not uniform and that there is a clear preference of the neutrons to be emitted in the forward direction. The effect is enhanced for highest neutron energies. However, if only small emission angles of the neutrons are considered ($\theta \ll 1^\circ$), the overall effect can be treated as a global normalisation between the number of neutrons emitted in all θ directions and the neutrons emitted with $\cos(\theta)$ values close to 1. The lower right corner of Figure 2 shows the ϕ distribution for neutron energies between 100 MeV and 1 GeV. It can be seen that these neutrons are emitted more likely in the $\phi = 90^\circ$ direction of the proton beam. The tendency is enhanced for neutrons above 1 GeV, which has the positive consequence of reducing the background produced by them close to the experimental area, situated 185 m downstream. However, the ϕ distributions for neutron energies below 100 MeV present a uniform behaviour. This allowed parameterising the neutron source to first order as the product of the single-variable distributions depending on the energy for the purpose of an *event generator*.

3. The beam optics

The optical elements of the installation are the beam pipe and the collimating system. The beam pipe defines the interaction-free transport medium where the neutrons can travel in vacuum up to the experimental area. A telescopic design was adopted for the pipe so that the tube does not intercept the neutrons arriving at the measuring station (185-200 m downstream): i) a first section being 70 m long with 80 cm diameter, ii) a second section being 68.4 m long with 60 cm diameter, and iii) a third section being 61.4 m long with 40 cm diameter. On the other hand, the collimating system is of fundamental importance as a background reduction element (shielding) and for providing a neutron beam of well defined size.

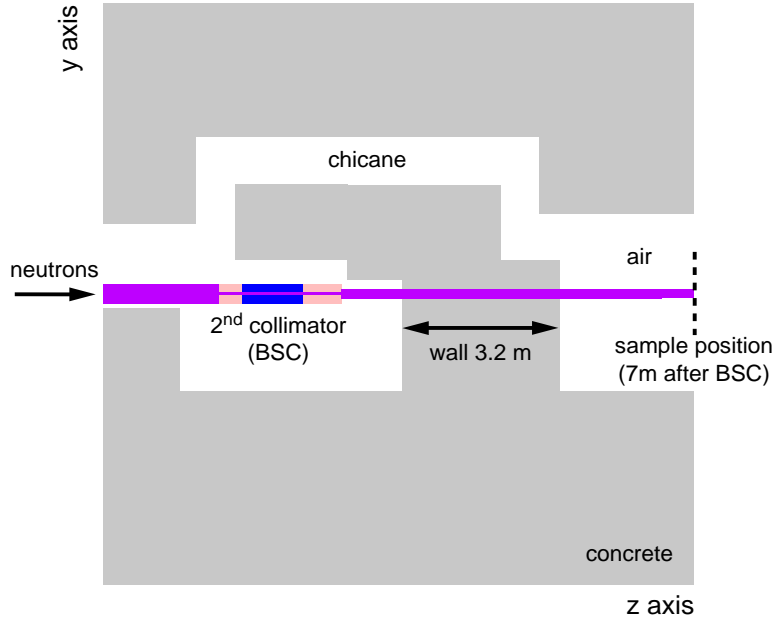
Table 1. Parameters of the two collimators. The z co-ordinates are referred to the exit face of the Pb target. The samples are assumed to be placed at $z = 185$ m, where the beam has a spread of 2 cm radius or 4 cm diameter.

Design of the first collimator						
	Material	Internal radius (cm)	External radius (cm)	Initial z coordinate (m)	Final z coordinate (m)	Length (m)
Part 1	Iron	5.5	25	135.54	136.54	1
Part 2	Concrete	5.5	25	136.54	137.54	1
Design of the second collimator						
	Material	Internal radius (cm)	External radius (cm)	Initial z coordinate (m)	Final z coordinate (m)	Length (m)
Part 1	5% borated Polyethylene	0.9	20	175.35	175.85	0.5
Part 2	Iron	0.9	20	175.85	177.1	1.25
Part 3	5% borated Polyethylene	0.9	20	177.1	177.85	0.75

From pure geometrical considerations, it can be realised that a beam of 2-cm radius at 185 m can be prepared if and only if the spallation target has a lateral size of almost 20 cm. This can be achieved by the use of an additional collimator which partially screens the Pb target. It should be pointed out that the spallation target should be considered an object consisting by two parts of the same material. A central cylindrical part of 20 cm radius representing the main part of the Pb spallation source is surrounded by an Pb reflector forming thus together an object of 40 cm radius, the actual TOF target. The advantages of Lead as spallation source and efficient reflector are well established [10]. It has been observed by Monte Carlo simulations that the neutron flux at energies below 1 MeV is increased about 50% due to this Pb reflector. The source screening by the additional collimator reduces the neutron flux, since the complete Pb target is no longer visible from the sample position through both collimators. However, this effect is less significant as naively expected, because the spatial distribution of the emanating neutrons is not uniform, but peaked at the centre of the Pb target. Moreover, the use of two collimators turns out to be the most effective way of reducing the neutron and γ background in the experimental area. The screening of the neutron source reduces by one order of magnitude the number of neutrons hitting the second collimator, which represents the strongest source of background observed therein.

The position and inner diameter of the two collimators were optimised [11] by minimising the losses in flux and by leaving the possibility of future upgrades (already under study) open. In particular, the study considered explicitly a first collimator that is also appropriate for producing neutron beams of 8 cm diameter (or even broader). The optimal configuration is described in Table 1. The first stage consists of a 2 metres long collimator (Source Screening Collimator, SSC) at 135.54 m from the Pb target and with an inner aperture of 5.5-cm radius. The second stage is a 2.5-m long collimator (Beam Shaping Collimator, BSC) at 175.35 m from the Pb target and with an inner aperture of 0.9-cm radius. Such a configuration provides a neutron beam of 4-cm diameter at the sample location, 185 m downstream from the Pb target.

Figure 3. Top view of the area where the BSC is located

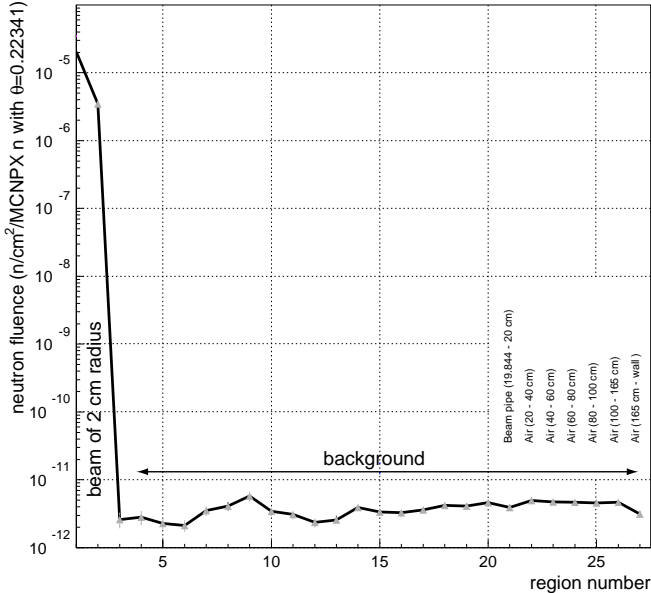


The optimal composition of the collimators was investigated as a separate issue by Monte Carlo simulations [2,3,4]. The best results were achieved when a combined or “sandwich-like” collimator is used [12]. In order to moderate the neutrons with energies below 20 MeV, a 40-50 cm long segment made of an hydrogen-rich compound doped with a neutron absorber (borated polyethylene – CH_2^{B} – in our case) was found to be very efficient. On the other hand, the neutrons above 20 MeV can not be efficiently stopped in CH_2^{B} . A 1 m long segment of an intermediate Z material (natural iron in our case) was found to be necessary and optimal for moderating, through elastic and inelastic scattering, the high-energy part of the TOF spectrum. For this reason, the SSC consists of a 1 m of iron and a 1 m of concrete cylindrical segments. A much more careful design was made for the BSC, only 5-7 m away from the measuring station, where the lowest background rates are required. Thus, a design based on three segments was adopted. The first part of the BSC, made of 50 cm of CH_2^{B} moderates and captures most of the neutrons below 20 MeV. The second part, made of 1.25-m iron, moderates and diffuses the high-energy neutrons below 20 MeV. The third part of the BSC, made of 75 cm of CH_2^{B} moderates and captures the neutrons scattered in the preceding iron segment.

4. The shielding elements

Several shielding elements have to be placed outside the TOF tube in order to bring the background at the experimental area to an optimal level. It has been observed by Monte Carlo simulation that it is of crucial importance to avoid high-energy neutrons (above several tens of MeV) reaching the vicinity of the experimental area and produce secondary particles. Thus, the best strategy is to take profit of the geometrical factor, by placing the shielding elements as far away as possible from the measuring station.

Figure 4. Radial distribution of the neutron beam profile and the neutron background at the sample position. The values correspond to the neutron fluence through concentric cylinders: the first 20 cylinders with radial increments of 1 cm and the last 7 as indicated in the figure.



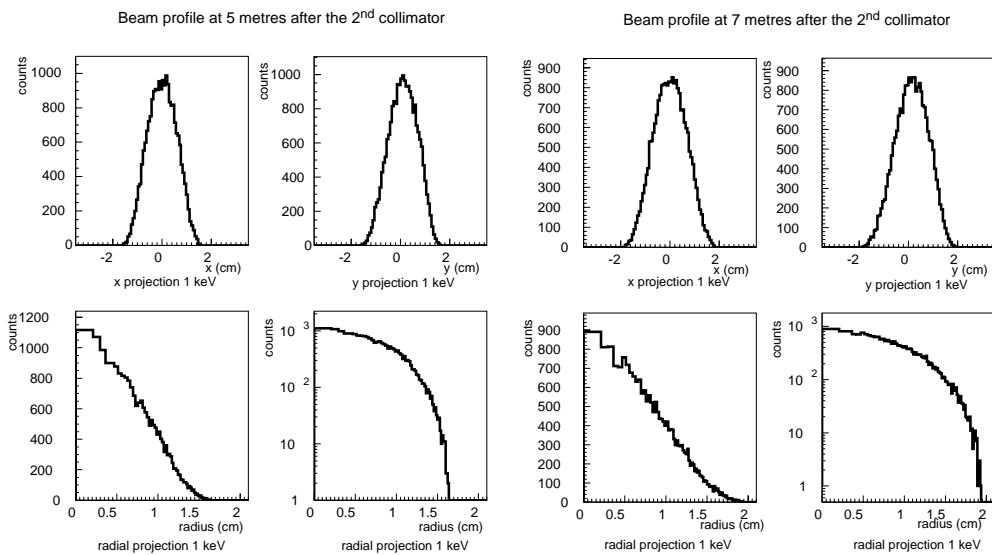
The first important shielding element is the pipe itself. Several tens of metres after the Pb target, the incidence angle of the neutrons hitting the pipe is small and the effective length of material seen by the neutrons is large. In this way, a large fraction of the neutrons are deviated from its initial trajectory and produce background in the upstream half of the tunnel. Due to the telescopic structure of the pipe, the places at the diameter reductions (80 cm to 60 cm and 60 cm to 40 cm) should be reinforced, since the neutrons traverse the pipe almost perpendicularly. At these positions, the pipe was covered after the reduction with 1-m thick external iron cylinders.

The second important shielding element is the first collimator (SSC) starting at 135.54 m. Such a strong scattering centre had to be shielded by a 3 m concrete wall. After the SSC, the neutron beam divergence is small and the neutrons do not hit the pipe before the second collimator (BSC). The 2.5 m long BSC diffuses and moderates very efficiently the whole neutron spectrum. However, it is a strong scattering centre that has to be efficiently shielded by a 3.2-m thick wall, placed 1 m beam-downstream. Figure 3 shows the top view of the area in scale, where the BSC is located, as has been designed for the MCNPX simulations. The 2.5-m long BSC is observed on the left-hand side of the 3.2-m concrete wall. Also visible is the chicane, a necessary escape path in case of emergency. The impact of this shielding opening on the background at the sample position was studied with Monte Carlo simulations.

The neutron beam profile and background at the sample position is shown in Figure 4. All the values correspond to the neutron fluence of concentric cylinders: the first 20 values with radial increments of 1 cm and the last 7 as indicated in the figure. The first two bins correspond to the main neutron beam, which has a radius of 2 cm. The remaining bins correspond to the background level at the different places. It can be seen that the neutron background is on average at the level of $2 \cdot 10^{-12}$ n/cm² per neutron emitted from the Pb target with a θ angle smaller than 0.223°. Such a value, when compared to the beam fluence of $2 \cdot 10^{-5}$, leads to a background to signal ratio of 10^7 . This background level is of the same order than the background of scattered neutrons produced at 15 cm from a 10 mg ²³⁵U sample placed in-beam. A similar result was found for the γ background produced

by neutron reactions. The level reached at a separation of 7 metres from it is 10^{-7} times smaller than the neutron beam shown in level by another by factor of ten. Such a value is comparable to the gammas emitted by a 10 mg ^{235}U sample. At 15 cm distance, the γ fluence is also seven orders of magnitude below the neutron beam fluence. As a general remark, it should be noticed that applying the necessary time of flight cuts would reduce the background levels shown in this section. In addition, several possibilities of reducing the neutron and γ background in the experimental area were also investigated. From the Monte Carlo simulations with GEANT and MCNPX, it was early observed that covering the walls with some neutron moderator and γ shielding could diminish the background level by another factor of ten.

Figure 5. Various projections of the beam profile at 5 and 7 metres after the BSC's for 1 keV neutrons



5. The beam at the experimental area

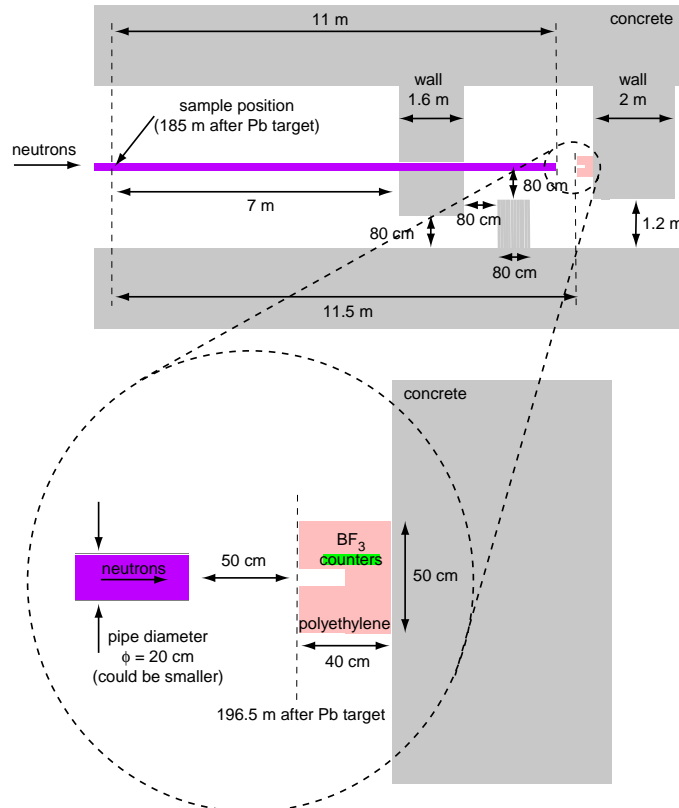
The neutron beam at the first phase of the n_TOF operation will have a maximal spread of 2-cm radius. Although the maximal size of the beam does not depend on the neutron energy, due to the energy dependence of the neutron spatial distributions at the exit of the Pb target, the beam profile at the sample position does also depend on the energy. The beam profile has been calculated by the geometric transport through the collimators for different neutron energies. Figure 5 shows various projections of the beam profile for 1 keV neutrons at several positions after the BSC. It can be observed from the radial projection in Figure 5 how the beam spread at 7 m after the BSC's end is inside the desired limit of 2 cm. However, it should be noticed that 5 m after the BSC, the beam spot is smaller and has a diameter of 3.2 cm. Thus, it remains to the particular experiment to decide which beam size has to be adopted.

It has been calculated by Monte Carlo simulations (FLUKA [2]) that for a PS bunch of $7 \cdot 10^{12}$ protons, the fluence in absence of collimators is of $7 \cdot 10^5 \text{ n/cm}^2$. With the described collimating system, the fluence amounts to $1.3 \cdot 10^5 \text{ n/cm}^2$ per proton bunch, which is smaller by a factor of 5. It should be emphasised that this loss in fluence is sine qua non to the definition of a neutron beam and a TOF facility fulfilling the requirements and providing the clean conditions necessary for experimentation.

6. The neutron escape line

The common experimental situation is that most of the neutrons in the beam do not interact with the samples. They continue its path undisturbed until it is finally interrupted by any interposed construction element. Such neutrons are a potentially dangerous source of background, since their interactions with the surrounding materials in the vicinity of measuring station can interfere with the experiments. It is necessary that they continue unperturbed its travelling for a long distance before being scattered. A typical solution adopted at other TOF facilities is to have an experimental area of large dimensions (several tens of metres). There the neutrons can travel (in air or vacuum) a long path before being scattered and finally absorbed. In addition, the background introduced by them can be highly suppressed by the TOF tagging, since the escape path is usually comparable (or larger) in length than the TOF distance.

Figure 6. Geometry of the neutron escape line as included in the MCNPX simulations



However, the particular situation at the n_TOF makes the mentioned strategies difficult to be applied. First, the facility is located inside a small closed cave, which limits severely the size of the experimental area. Second, the TOF tube hits the ground at 200 m from the Pb target, just 15 m after the measuring station. This situation introduces an unavoidable source of background close to the measuring station. Third, such a distance is much smaller than the 185 m TOF flight path, which affects the suppression capabilities of the time tagging. Fourth, the high-energy component of the neutron energy spectrum. All this considerations make preferable to design a neutron escape line and a beam dump at its end (properly shielded) instead of having the uncontrolled collision of the neutron beam with the floor at 200 m. Additional motivations for the neutron escape line from radio-protection considerations have not been studied.

The geometry of the beam dump proposed and included in the simulations can be seen in Figure 6. At the leftmost part of the figure, the sample position at 185 m from the Pb target is marked by a dashed line. After it, the unperturbed fraction of the neutron beam continues its travelling in vacuum for another 11 m, inside an aluminium pipe. It is worth to mention that the tube considered in our study has a diameter of 20 cm, which is larger than really necessary. As it is shown in Figure 6, the neutron beam has a maximal spread of 8 cm diameter at 200 m, which would allow the use of a smaller pipe diameter. However, in order to make sure about the conclusions, it is preferable to know that the number of neutrons backscattered at the beam dump is even acceptable for a broader tube (larger geometric acceptance).

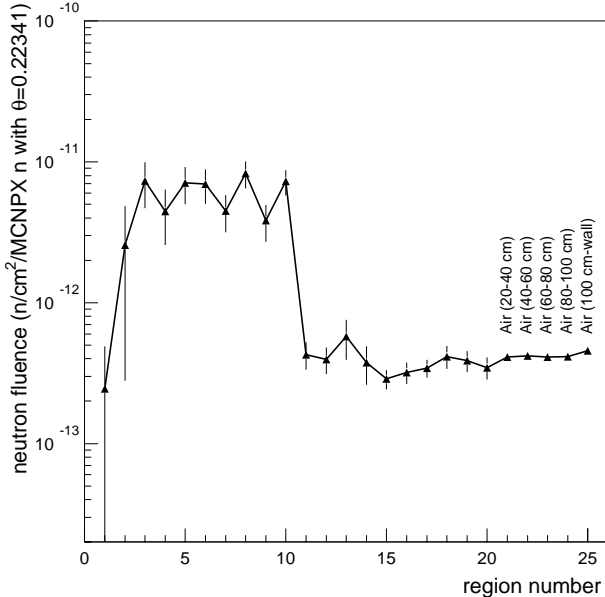
After the 11 m flight path, the neutrons cross a 1 mm thick tube end cup and enter into air. Several materials for the tube end cup have been studied: 1 mm of Al, 1 mm of natural Fe, 1 mm of carbon fibre and also the ideal case of no end cup (only vacuum). The MCNPX [3] Monte Carlo simulations revealed no influence of the end cup election on the background distribution at the sample position.

After the vacuum pipe and 50 cm of air, the neutrons first enter into a $40 \times 50 \times 50$ cm³ polyethylene block followed by a 2 m thick concrete wall. The polyethylene block has two main purposes. First, it preferences the scattering of the neutrons in the forward direction, thus reducing the background in the upstream area. Second, it is the frame for a monitoring detector array based on three BF₃ detectors. The 2-m thick concrete wall behind the polyethylene block is in charge of further moderation and absorption of the neutrons. Only the neutrons of highest energies, above several tens of MeV are capable to cross it.

In order to minimise the number of scattered neutrons entering back into the experimental area, a 1.6-m thick concrete wall is interposed in their way. The wall is placed at 7 m from the sample position, as far as possible from the point of view of the neutron and γ background. Also visible in Figure 6 is the 80 cm broad opening in the wall, necessary from the point of view of safety. Nevertheless, the opening is covered by an additional 80-cm thick concrete shielding forming a chicane. By keeping the distance of this shielding to the centre of the pipe, also 80 cm, the neutrons can go through the wall opening only after having suffered more than one interaction.

It should be said at this point that the geometry of the tunnel described in Figure 6 is only an approximation to the real one. The curvature of the tunnel and its slope were not included. However, if the distances marked in the figure are kept as they are, the results for the real geometry must be the same or better, since the approximations made were always done by following the tendency of increasing the background at the experimental area. Moreover, the geometry described in Figure 6 allows further improvements, because the dimensions of the present shielding elements are not at its practical limits. For example, there is still space for enlarging them or moving all the shielding elements 2 metres away from the sample position. However, the present configuration provides already satisfactory results.

Figure 7. Neutron background at the sample position. The values correspond to the neutron fluence through concentric cylinders: the first 20 cylinders with radial increments of 1 cm and the last five as indicated in the figure.



The lower part of Figure 6 is an enlarged view of the beam dump at the end of the neutron escape line. Three commercially available BF_3 detectors are embedded on the polyethylene block forming a long counter [13]. The hole of 4-cm radius is only necessary for the BF_3 long counter working principle. The main goal of this monitoring set-up is to control possible variations in the gross properties of the neutron beam such as its intensity or its position. Figure 7 shows the radial distribution of the neutron background at the sample position. All the values correspond to the neutron fluence through concentric cylinders: the first 20 values with radial increments of 1 cm and the last five outside the pipe as indicated in the figure. Such a background can be compared directly to the previously shown in Figure 4. Two different components can be observed. The first one corresponds to the initial 10 bins and accounts for the neutrons scattered at the beam dump and travelling back inside the pipe. Such a background can be considered as a negligible contamination of the beam of 1 part in 10^6 (see Figure 4 to compare with the main beam). A suppression if this background can be achieved by placing a sheet of Cd in front of the polyethylene block. The second component is the neutrons travelling outside the pipe, which arrived at the experimental area either by crossing the tube hole or the opening in the wall. This background is at the same level as the one in Figure 4, that is, seven orders of magnitude below the main neutron beam. The energy distribution of the background at the sample position shows that 95% of the neutrons have energies below 1 eV. In order to investigate if such neutrons are coming from the moderation of higher energy neutrons or had initially thermal energies, a Monte Carlo simulation was performed with an energy spectrum starting at 1 eV. The result is that 53% of the thermal neutrons at the sample position are produced by neutrons of energies higher than 1 eV. The other 47% is already originated by neutrons with initial thermal energies. This implies additional background suppression because the neutron energy spectrum at the sample position is affected at energies below 0.1 eV because of gravitation. In fact, gravitation will make that the thermal neutrons emitted from the Pb target fall down along the TOF path of 200 m and do not reach the samples. The Monte Carlo simulations revealed also that at the sample position, the γ background due to the beam dump is at least 7 orders of magnitude below the main neutron beam.

REFERENCES

- [1] S. Abramovich *et al.*, *Proposal for a Neutron Time of Flight Facility*, CERN/SPSC 99-8, (March 1999).
- [2] A. Ferrari and P.R. Sala, *Intermediate and High Energy Models in FLUKA: Improvements, Benchmarks and Applications*, Proc. of Int. Conf. on Nuclear Data for Science and Technology, NDST-97, ICTP, Miramare-Trieste, Italy, May 19-24 (1997).
- [3] Laurie S. Waters, Editor, *MCNPX Users Manual*, TPO-E83-G-UG-X-00001, Los Alamos National Laboratory (1999).
- [4] GEANT3, *Detector Description and Simulation Tool*, CERN Program Library W5013, Geneva (1994).
- [5] GEANT4, <http://wwwinfo.cern.ch/asd/geant4/geant4.html>.
- [6] C. Coceva, M. Magnani, M. Frisoni, A. Mengoni, *CAMOT: a Monte Carlo Transport Code for Simulations of Pulsed Neutron Sources*, Unpublished (2000).
- [7] H. Arnould *et al.*, *Neutron-driven Nuclear Transmutation by Adiabatic Resonance Crossing: TARC*. EUR 19117. Project Report of the NST of EURATOM of the EC. ISBN 92-828-7759-0 (1999).
- [8] E. Radermacher, Editor, *Neutron TOF Facility (PS 213) – Technical Design Report*, CERN (February 2000).
- [9] D. Cano-Ott *et al.*, *First Parameterisation of the Neutron Source at the n_TOF and its Influence on the Collimation System*, DFN/TR-03/II-00.
- [10] H. Arnould *et al.*, *Experimental Verification of Neutron Phenomenology in Lead and Transmutation by Adiabatic Resonance Crossing in Accelerator Driven Systems*. Phys. Lett. B 458 (1999) 167.
- [11] D. Cano-Ott *et al.*, *Proposal for a Two-step Cylindrical Collimator System for the n_TOF Facility*, DFN/TR-04/II-00.
- [12] D. Cano-Ott *et al.*, *Design of a Collimator for the Neutron Time of Flight (TOF) Facility at CERN by Means of FLUKA/MCNP4b Monte Carlo simulation*, DFN/TR-07/II-99.
- [13] A.O. Hanson and M.L. McKibben, Phys. Rev. 72, 673 (1947).

